JOURNAL OF Applied Polymer SCIENCE

Structure, Properties, and Mechanism of Reactive Compatibilization of Epoxy to Polyphenylene Sulfide/Polyamide Elastomer

Hao Gui , Tao Zhou , Lin Li , Ting Zhou , Feiwei Liu , Yanhui Zhan , Aimin Zhang
State Key Laboratory of Polymer Materials Engineering of China, Polymer Research Institute, Sichuan University, Chengdu 610065, China
Correspondence to: T. Zhou (E-mail: zhoutaopoly@scu.edu.cn) or A. Zhang (E-mail: amzhang215@vip.sina.com)

ABSTRACT: In this article, the structure, properties, and mechanism of reactive compatibilization of epoxy (EP) to polyphenylene sulfide (PPS)/polyamide elastomer (PAe) were investigated in detail. A PPS/PAe/EP ternary system was successfully prepared via reactive extrusion. Its mechanical and rheological properties were greatly improved compared with those of conventional PPS/PAe binary system. The addition of EP to PPS/PAe blend induced a series of chemical reactions. The chain-extended reaction of PPS was verified by high pressure capillary rheometer. The grafting reaction of PPS with PAe was testified by FTIR. The curing reaction of EP was proposed to explain the decreasing of the mechanical properties in PPS/PAe/EP ternary blend when it contained a high content of EP. Additionally, a toughened model was also proposed in PPS/PAe/EP ternary system. The improvement of toughness was attributed to the activation of matrix molecules in the shear band region. © 2013 Wiley Periodicals, Inc. J. Appl. Polym. Sci. 000: 000–000, 2013

KEYWORDS: blends; compatibilization; elastomers; properties and characterization

Received 9 January 2013; accepted 27 May 2013; Published online
DOI: 10.1002/app.39610

INTRODUCTION

Polyphenylene sulfide (PPS) has excellent mechanical properties, electrical insulation, chemical resistance, flame resistance, radiation resistance, thermal stability, and dimensional stability.[1–3] Therefore it is widely used as electronic, electrical, automotive, precious molded and mechanical articles.[3] However, the brittleness of PPS, which is due to the rigid backbone and the crosslinking architecture, greatly restricts its applications.

In order to make up for this demerit, there have been some studies on the chemical modification of PPS, such as introducing of flexible spacers in the rigid PPS main chain or grafting of flexible spacers on that. Some physical modifications,[1–13] for example blending PPS with other polymers, were also studied. Usually, the former method is very difficult to achieve and it requires a long process time. Moreover, even though achieved, it can adversely affect the intrinsic advantageous properties of PPS. However, the latter method is much easier to achieve and it is in line with the requirement of large-scale industrialized fabrication.

Sugie et al.[1] studied ternary or quaternary compounds which consisted of PPS, epoxy (EP), other thermoplastics, and (or) reinforced fillers. The EP only served as chain extender for PPS. Chen et al.[4] successfully prepared the epoxide group modified polyethylene-glycidyl methacrylate (PE-GMA) from GMA and low-density polyethylene (LDPE) via the grafting reaction of extrusion. As a compatibilizer for PPS/PA66/GF (glass fiber) blend and PPS/poly(ethylene terephthalate) alloy, the PE-GMA greatly improved the mechanical properties of those compounding systems. Choi et al.[2] focused on the PPS/PC/EP ternary system. The tensile properties of PPS/PC/EP were obviously improved due to the homogeneous morphology and the suppression of polycarbonate decomposition by adding a small amount of EP to PPS/PC system. Lee and Chun[3] found that 95 wt % PPS/5 wt % poly(ethylene-*stat*-glycidyl methacrylate)-*graft*-poly-(acrylonitrile-*stat*-styrene) (EGMA) blend achieved the highest tensile strength and impact strength.

Generally speaking, in order to improve the impact strength of brittle polymers, it is common to add elastomer or tough polymers[3] to matrix, expecting craze and plastic deformation of matrix. In industry, polyamide and PPS have been successfully blended due to their similar polarity and compatibility. Considering both of the above mentioned points, polyamide elastomer (PAe), with the hard segment of polyamide 12, can be expected to be somewhat compatible with PPS, and it is a proper elastomer to toughen PPS. Even though the miscibility is not always desirable in polymer blends, a satisfactory adhesion between both phases must be required to obtain a good mechanical property.[2] Reactive extrusion is an easy way for industrial production. And the twin-screw extruder has an excellent melt

Applied Polymer SCIENCE

Table I. The Formula of the Ternary Blends

Samples	PPS	PAe	EP
PPS-0-10	100	10	0
PPS-1-10	100	10	1
PPS-2-10	100	10	2
PPS-3-10	100	10	3
PPS-4-10	100	10	4
PPS-5-10	100	10	5
PPS-6-10	100	10	6
PPS-7-10	100	10	7

blending effect and a high shear strength. So the reactive extrusion for PPS/PAe/EP ternary system by a twin-screw extruder was employed.

In this study, a low-molecular-weight EP was directly introduced to PPS/PAe blend, which was studied by few researchers. The PPS/PAe/EP blends had excellent mechanical properties and improved rheological properties compared with the EP-free counterpart. The rheological properties of blends were measured by high pressure capillary rheometer. The mutual chemical reactions among PPS, PAe, and EP were verified by attenuated total reflectance Fourier transform infrared spectroscopy (ATR-FTIR). The mechanical properties of blends were studied by tensile and impact test. Using scanning electron microscope (SEM), the dispersed particle size, size distribution, and morphology in blends were clearly observed. Whereafter a toughened model was proposed to explain the above results. Finally, to evaluate the thermal properties, the glass transition temperature and the decomposition temperature of blends were tested by dynamic mechanical analysis (DMA) and thermogravimetric analysis (TGA), respectively.

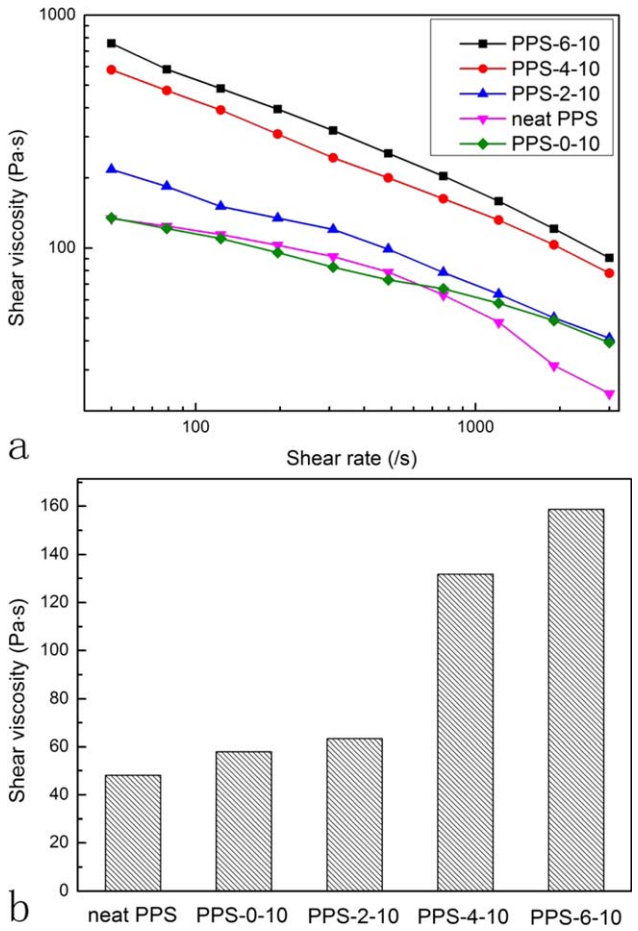

Figure 1. The relationship between shear viscosity and shear rate of neat PPS, PPS-0-10, PPS-2-10, PPS-4-10, and PPS-6-10 (a) and the shear viscosity of neat PPS, PPS-0-10, PPS-2-10, PPS-4-10, and PPS-6-10 at the shear rate of 1208.5/s (b) at 295°C. [Color figure can be viewed in the online issue, which is available at wileyonlinelibrary.com.]

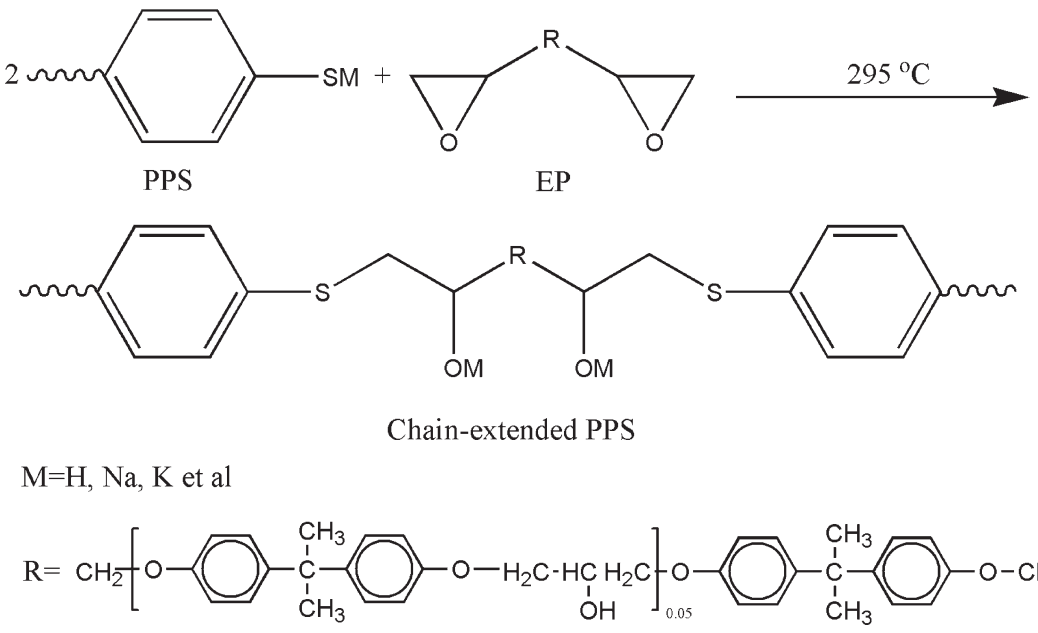

Scheme 1. The chain-extended reaction of PPS in the presence of EP.

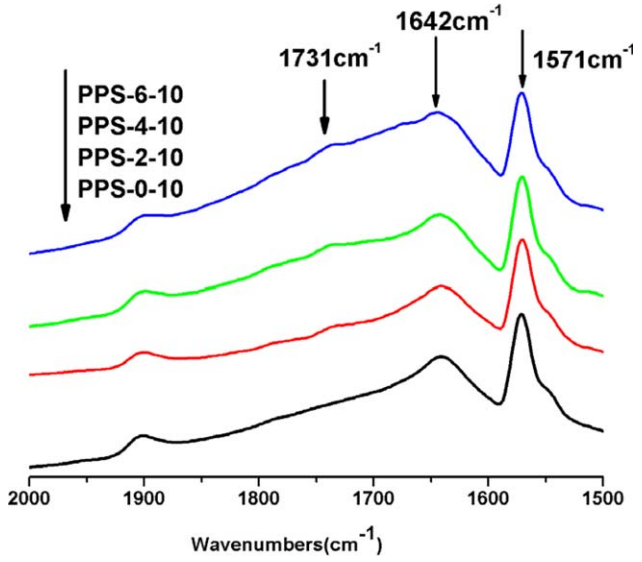

Figure 2. FTIR-ATR spectra of PPS-0-10, PPS-2-10, PPS-4-10, and PPS-6-10. [Color figure can be viewed in the online issue, which is available at wileyonlinelibrary.com.]

EXPERIMENTAL

Materials

In the present study, the partially crosslinked PPS (PPS-HB DL, Sichuan Deyang Chemical Co., Ltd, Chengdu China), with a weight average molecular of 40,000–50,000 g/mol and a melt flow rate of less than 180 g/10 min, was used. The PAe (Pebax 6333, Arkema, France), which is a multi-block linear polymer, with the soft segment of polytetramethylene ether and the hard segment of polyamide 12, was used. The EP (DQ200E, Dongfang Turbine Co., Ltd, Deyang China), with the epoxide number of 0.565 mol/100 g, was also employed.

The formula of PPS/PAe/EP ternary blends is shown in Table I. Taking PPS-4-10 as an example, EP was 4 phr by weight and PAe was 10 phr by weight compared with PPS. Before experiments, PPS and PAe were dried for 4 h in a vacuum oven at 110°C and 75°C respectively.

Reactive Extrusion and Injection Molding

Taking PPS-4-10 as an example, PPS, PAe, and EP were mixed in a high-speed mixer (rotating speed = 25,000 rpm, mixing time = 20 s) according to the formula from Table I. Then the mixtures were fed to a co-rotating twin-screw extruder (D = 21 mm, L/D = 32:1) at 180 rpm. The processing temperature was between 285°C and 295°C. The extrudate was cooled through a stainless steel sink and then it was pelletized. After being dried for 4 h at 110°C in a vacuum oven, the pellets were fed to an injection molding machine (K-TEC40, Ferromatic Milacron, Germany) to shape the measured specimens. The temperature from feed to nozzle was 50, 285, 295, 300, 305°C and that of mold was room-temperature. The injection pressure was 60 MPa and the plasticizing stroke was 70 mm. The preparation of the other blends was identical to that of PPS-4-10.

Table II. The Bands Assignment of Blends[14]

Wavenumber (cm^{-1})	Assignments
1571	the skeletal vibration of benzene ring in PPS
1642	the peak combining the C=O stretching of the amide group in PAe at 1636 cm^{-1} with the overtone of C—H off-plate bending attached to benzene ring in PPS at 1648 cm^{-1}
1731	the C=O stretching of the ester group in PAe

Rheological Testing

The rheological properties of pure PPS, PPS-0-10, PPS-2-10, PPS-4-10, and PPS-6-10 were measured using the piston-mode Rosand RH70 (Malvern, Bohlin Instruments, Britain) capillary rheometer at 295°C. The capillary has a die diameter of 1.0 mm and a length-to-diameter ratio of 16.

Chemical Reactions Analysis

Firstly, the PAe of PPS-0-10, PPS-2-10, PPS-4-10, and PPS-6-10, which did not react with PPS, was dissolved by hot sulfuric acid for more than 10 h. After being washed with lots of water and being dried in a vacuum oven, the surface of those samples was tested by ATR-FTIR (iS10, Nicolet, America).

Mechanical Properties Measurement

The uniaxial tensile test was carried out using a mechanical testing machine (CMT4101, Shenzhen SANS testing machine, Shenzhen China). The tensile crosshead speed was 5 mm/min, and the gauge length was 50 mm. The Charpy impact strength of unnotched rectangular bars (80 mm × 10 mm × 4 mm) was measured using an impact tester (XJU-22J, Chengde Testing Machine, Chengde China). The impact velocity of pendulum was 2.9 m/s. All the tests were carried out at room-temperature.

Particle Size and Size Distribution Observation

For observing the morphology of blends, the samples of PPS-0-10, PPS-2-10, PPS-4-10, and PPS-6-10 were fractured in liquid nitrogen. Then PAe was etched by hot sulfuric acid for 2 h. The dispersed particle size and the size distribution were observed by a SEM (JSM-5900LV, JEOL, Japan). All samples were coated with a thin layer of gold to increase the contrast.

Morphological Analysis of the Shear Yielding Zone

The microstructure of shear yielding zone was also observed by SEM. The shear yielding deformation was carried out by the uniaxial tensile test at a tensile crosshead speed of 1 mm/min. The deformed specimens were broken in parallel with the tensile direction at the center of the width. All samples were coated with a thin layer of gold before observation.

Dynamic Mechanical Analysis

A dynamic mechanical thermal analyzer (DMAQ800, TA, America) was used for measuring the temperature-dependent dynamic modulus. Test was conducted with three-point bending mode, and the support span was 20 mm. The testing temperature ranged from 40 to 210°C at a heating rate of 5 °C/min. In this experiment, the oscillation frequency was 1 Hz and the amplitude was 25 μm.

Applied Polymer SCIENCE

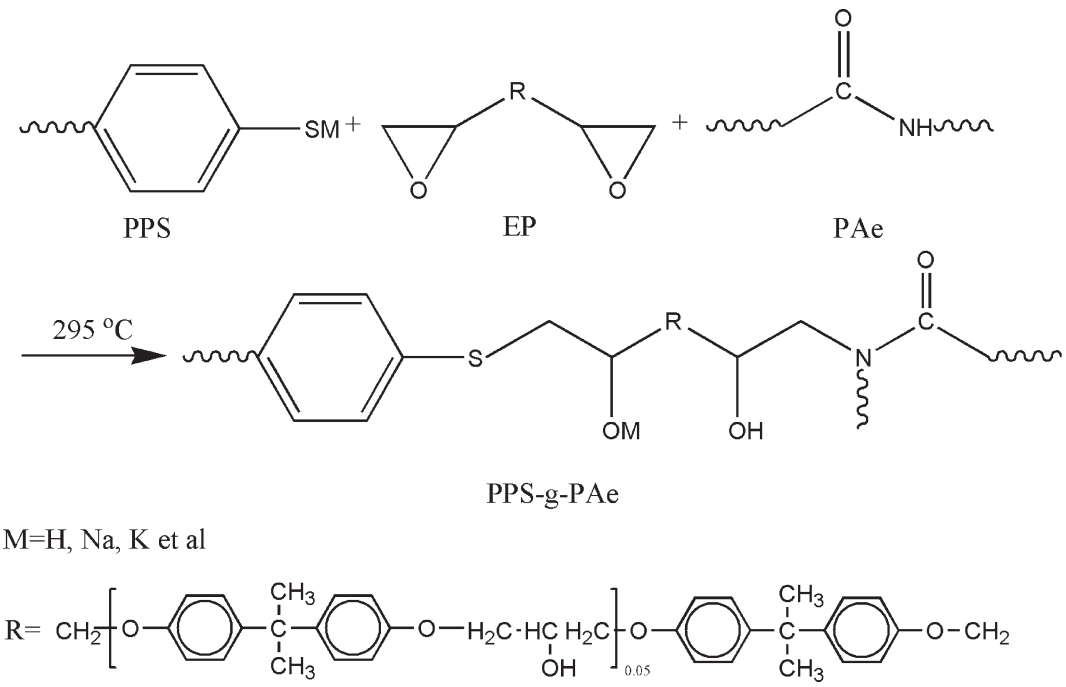

Scheme 2. The PPS-*g*-PAe reaction in the presence of EP.

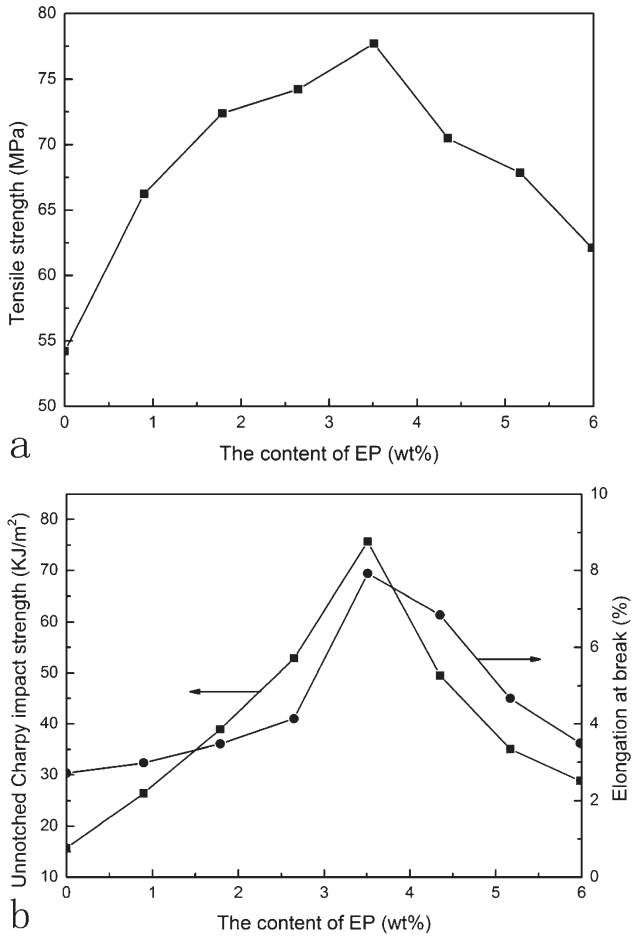

Figure 3. The tensile strength (a) and the unnotched Charpy impact strength and the elongation at break (b) of PPS/PAe/EP blends.

Thermal Analysis

In order to evaluate the thermal properties of blends, the decomposition temperature and the heat deflection temperature were measured. A thermogravimetric analyzer (TG209 F1, Netzsch, Germany) was used for comparing the thermostability of PAe, PPS, and PPS/PAe/EP blends. The testing temperature ranged from room-temperature to 800°C at a heating rate of 20 °C/min and nitrogen was used as purged gas. The heat deflection temperature was tested by a Vicat heat distortion temperature detector (HDV2, ATLAS, America) at a heating rate of 120 °C/h under a load of 1.82 MPa.

RESULTS AND DISCUSSION

Rheological Properties of Blends

Because of its low melt strength, conventional PPS resin is unsuitable for the extrusion and the blow molding. In this study, the high pressure capillary rheometer was used to evaluate the processing properties of blends. As shown in Figure 1(a), we find that all samples are in line with the shear-thinning characteristic. That is, with increasing shear rate, the shear viscosity decreases gradually. On the other hand, with increasing the content of EP, the shear viscosity of blends increases at a specific shear rate.

The most interesting characteristic is shown in Figure 1(b). The shear viscosity changes slightly when the content of EP ranges from 0 to 2 phr or from 4 to 6 phr. However, when the EP content is in the range of 2–4 phr, the shear viscosity has a sharp increase.

The impressive increasing of shear viscosity can be explained by the chain-extended reaction of PPS as displayed in Scheme 1. The added EP first selectively reacts with the chain end groups (—S^-M^+ or —SH, M^+ can be Na^+, K^+ etc.) of PPS, resulting

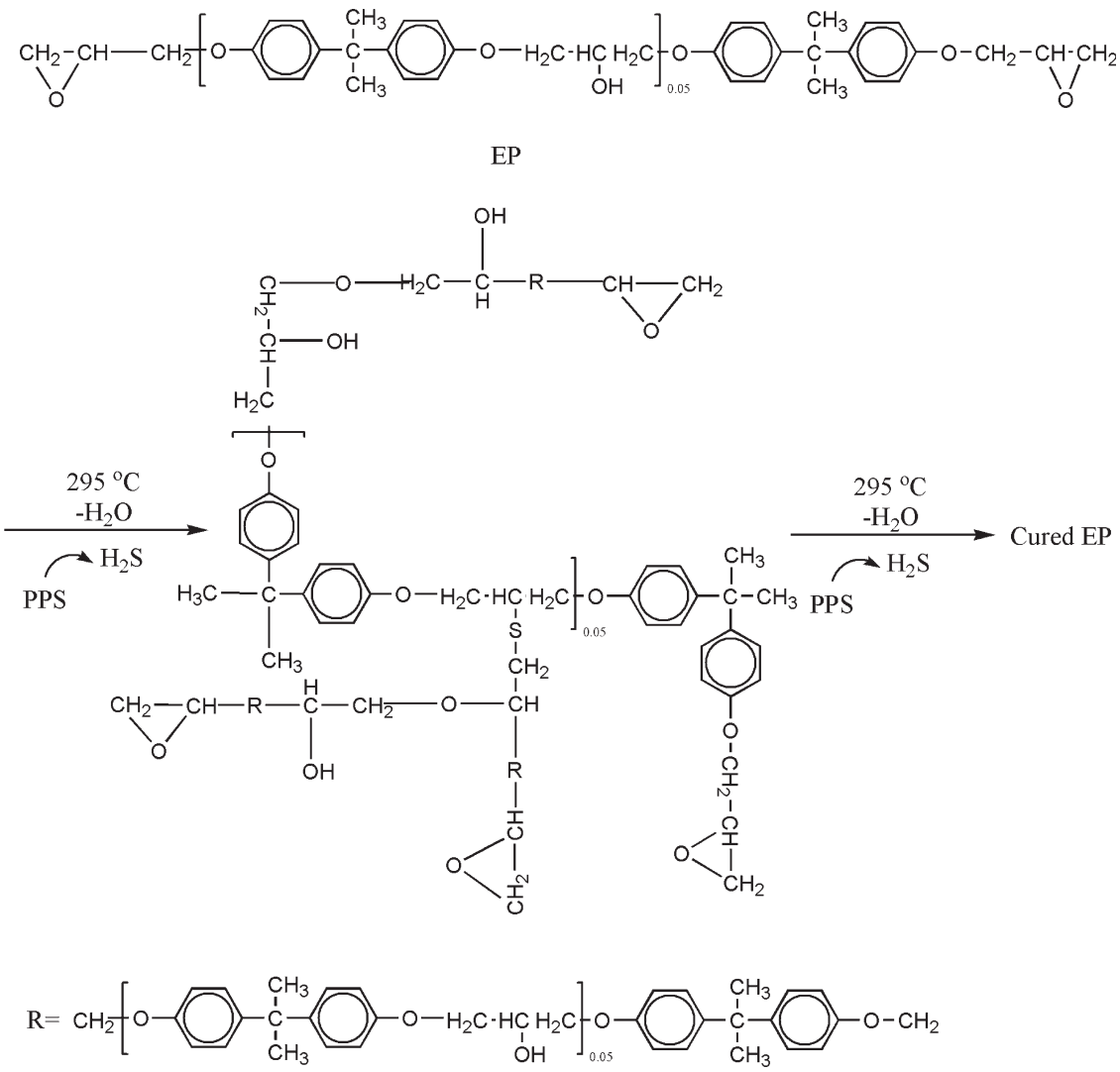

Scheme 3. The curing reaction of EP.

in a chain-extended PPS. Due to the improvement of PPS molecular weight, the increasing entangled effect changes the shear viscosity as shown in Figure 1(a). The interesting increase in viscosity as displayed in Figure 1(b) can be attributed to the sharp improvement of PPS molecular weight when the content of EP ranges from 2 to 4 phr. With further increasing EP content, there are almost no extra end groups of PPS reacting with EP, so the shear viscosity improves slightly.

ATR-FTIR of Blends

The ATR-FTIR spectra and the bands assignments of PPS-0-10, PPS-2-10, PPS-4-10, and PPS-6-10 are displayed in Figure 2 and Table II, respectively. As shown in Figure 2, the peaks at 1571 cm^{-1} are assigned to the skeletal vibration of the benzene ring of PPS, and their areas are almost identical. So they can be treated as the internal standard peaks. However, as the content of EP increases, the peaks at 1642 cm^{-1}, which are assigned to the peak combining the C═O stretching of amide group in PAe at 1636 cm^{-1} with the overtone of C—H off-plate bending attached to benzene ring in PPS at 1648 cm^{-1}, become broad, and their areas also increase. In addition, the peaks at 1731 cm^{-1}, which are assigned to the C═O stretching of ester group in PAe, develop from scratch, and their intensities do also strengthen. From the above phenomena, it can be concluded that the PAe grafted PPS copolymer (PPS-*g*-PAe) is really produced as displayed in Scheme 2.

When the mixtures are blended at 295°C, the amide groups of PAe which have some reactive activity can also react with the epoxide groups of EP, resulting in a PPS-*g*-PAe copolymer (shown in Scheme 2). It can be speculated that the PPS-*g*-PAe exists in the interphase between PPS and PAe and certainly improves their interfacial adhesion or compatibility. This provides a great benefit to the tensile strength and impact strength of the blends.

Mechanical Properties of Blends

Figure 3 shows the tensile strength, the unnotched Charpy impact strength, and the elongation at break of PPS/PAe/EP ternary blends. Obviously, all the properties have the same trends. First, they increase with EP up to 3.5 wt %. When the content of EP is 3.5 wt %, these properties reaches their maximum, i.e.

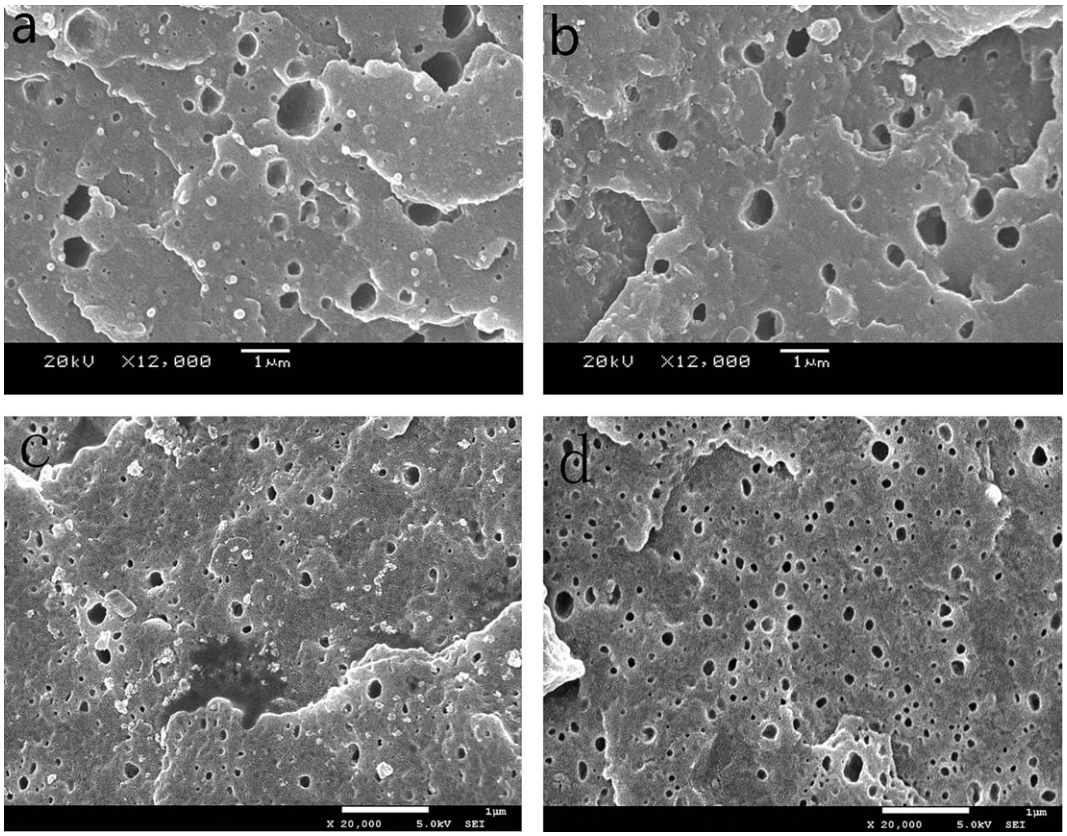

Figure 4. SEM micrographs of the fracture surface of PPS-0-10 (a), PPS-2-10 (b), PPS-4-10 (c), PPS-6-10 (d).

77.7 MPa, 7.93%, and 75.69 kJ/m^2, respectively. With EP increasing in further, they decrease adversely.

The fact that all these properties increase with EP up to 3.5 wt % can be interpreted as follows. Firstly, the chain-extended PPS (shown in Scheme 1) results in the increasing Van der Waals force and entangled effect among PPS molecular chains, which improves the tensile strength and the toughness. Secondly, the PPS-*g*-PAe copolymer enhances the interfacial adhesion between PPS and PAe, and so the tensile strength of blends increases to some extent. At the same time, the PPS-*g*-PAe decreases the interfacial tension and augments the interfacial area between PPS and PAe, which is beneficial to the improvement of impact strength due to the initiation of shear band on the interface.[15]

In order to explain the decline of mechanical properties when the EP exceeds 3.5 wt %, the curing reaction of EP is proposed as shown in Scheme 3. Due to the high temperature (295°C) and the outgassing (H_2S) from PPS during processing,[1,2] the curing reaction of EP can take place. Because of the immiscibility of PPS and cured EP, the cured EP acts as the stress concentration points which not only decrease the tensile strength but also make the blends brittle.

Dispersion of PAe in Blends and a Toughened Model for PPS/PAe/EP System

The cryogenically fractured surfaces of PPS-0-10, PPS-2-10, PPS-4-10, and PPS-6-10 are shown in Figure 4. The voids represent the PAe etched by hot sulfuric acid for 2 h. In the blends containing 0 and 2 phr EP [shown in Figure 4(a,b)], the average size (0.6 μm) and the size distribution of PAe are similar. The size distribution is so wide that the maximal diameter of dispersed particle is about 1 μm and the minimal one is less than 0.1 μm. This phenomenon is arisen from the immiscibility between PPS and PAe. When the content of EP is 4 and 6 phr [shown in Figure 4(c,d)], the PAe particles are well dispersed in PPS matrix, and the average particle size is about 0.1 μm. Adding EP to PPS/PAe blends significantly increases their compatibility.

Combining the experimental results (Figures 3 and 4) with the toughened theories in semicrystalline polymers by Kim et al.[15] and Wu,[16] we propose a toughened model for PPS/PAe/EP ternary system as shown in Figure 5. In this model, the micromechanical process is described as a three-stage-mechanism. Stage 1 is the stress concentration. Stage 2 is the voids and the shear band formation. Stage 3 is the induced shear yielding.

PPS-0-10 is a typical example for the left of Figure 5. The particle size is large due to the poor adhesion between dispersed particles and matrix. In the first stage, the stress concentrates around particles due to the different elastic properties between particles and matrix. With the strain increasing, the maximal stress occurs in the equatorial region of particles. Because of the poor adhesion, debonding (or voids) can easily take place on

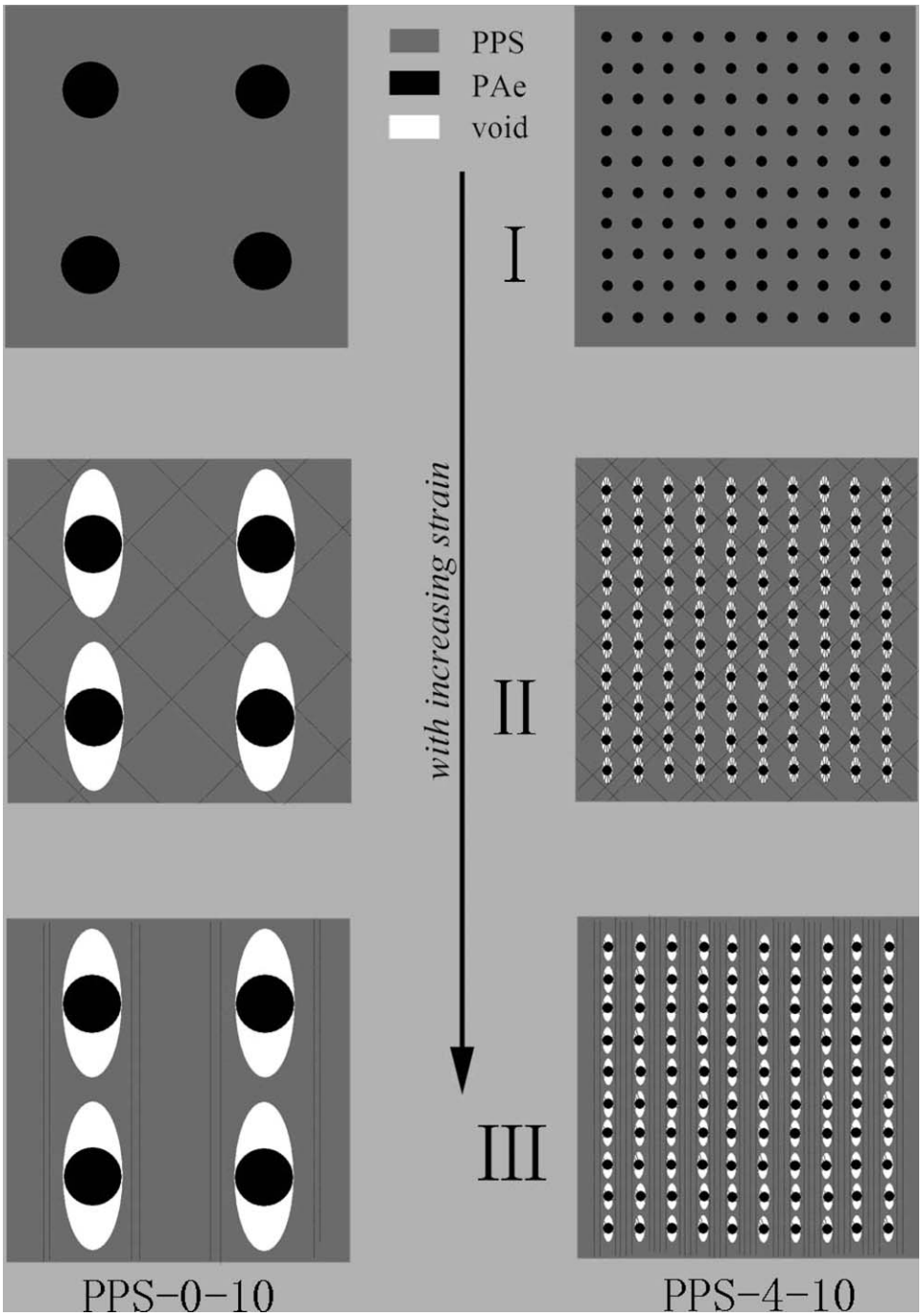

Figure 5. The toughened model for PPS/PAe/EP system.

both polar regions of the particles. At the same time, the shear bands form in the matrix at an angle of 45° to the direction of the maximum principal tensile stress (in the second stage). In the next stage, the matrix between particles is deformed through shear yielding.

Due to the PPS-*g*-PAe acting as a compatilizer for PPS and PAe in PPS-4-10, as displayed in the right of Figure 5, the particle size is greatly reduced. Firstly (Stage 1), the stress concentration occurs around particles. Secondly (Stage 2), fibrils probably form at the interface between dispersed particles and matrix due to the phase adhesion. Simultaneously, the shear bands also form in the matrix between particles. Thirdly (Stage 3), with the strain increasing, the fibrils break down at the polar regions of particles. Only a few fibrils remain in the area of the equatorial region of particles, and the shear yielding is induced in the matrix.

According to the rubber toughened theory proposed by Wu,[16] there existed a certain critical interparticle distance for a specific polymer. Above the critical distance, polymer blends characterized brittle; and less than the critical distance, polymer

Applied Polymer SCIENCE

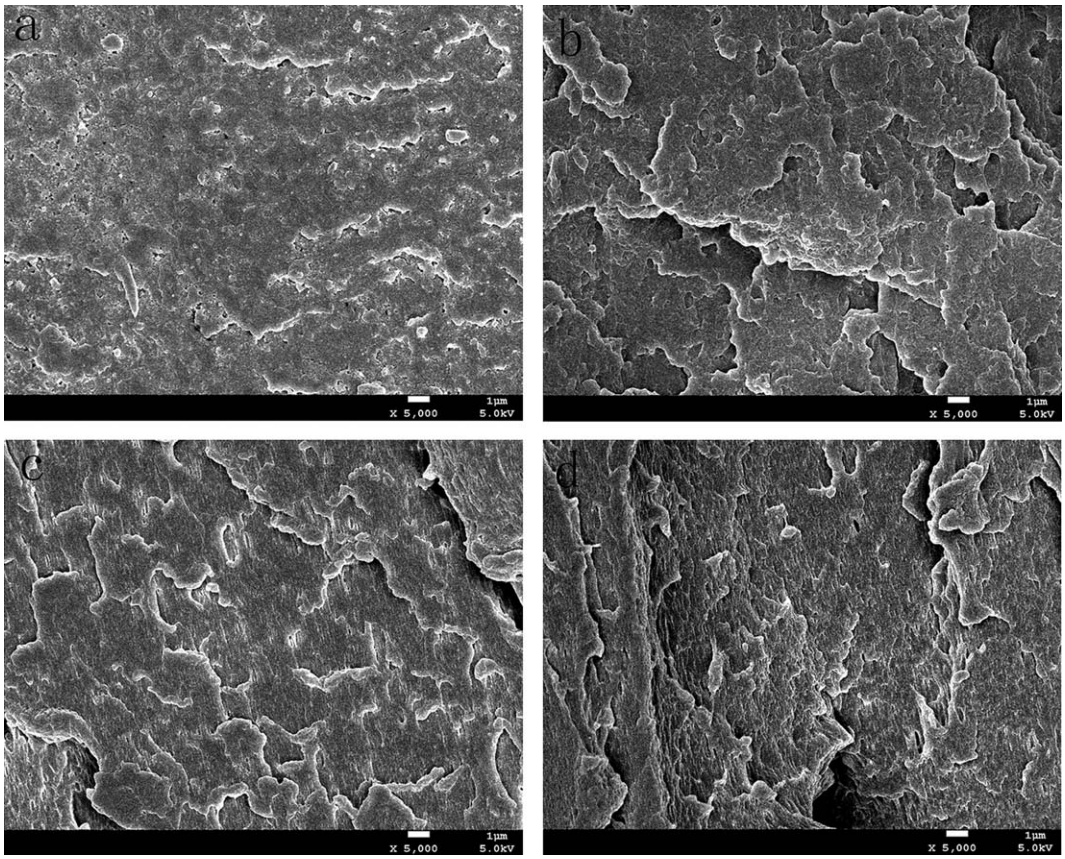

Figure 6. The microstructure of the shear yielding zone of PPS-0-10 (a), PPS-2-10 (b), PPS-4-10 (c), and PPS-6-10 (d).

alloys became tough. However, Wu did not provide the detailed explanation for the brittle-tough transition. As mentioned in Stage 2, the shear bands form around dispersed particles. We think that the region of shear bands is directly proportional to the superficial area of dispersed particles. The molecules within the region of shear bands, especially within the intersectional region, are more active than the others in matrix. So the yield strength of this band region is lowered, and the toughness of polymer blend is improved by the induced shear yielding.

In the present study, due to the poor adhesion between particles and matrix, the particle size of PPS-0-10 is so large that the active molecules of the band region in matrix are few. This practically reflects the low value of unnotched Charpy impact strength. Because of the forming of PPS-*g*-PAe, the particle size becomes much smaller in PPS-4-10. So the active molecules of the band region are throughout the matrix and the unnotched Charpy impact strength is increased greatly.

The toughened model can be directly proven by the experimental results as shown in Figures 6 and 7. In Figure 6, PPS-4-10 and PPS-6-10 have more yielding matrix compared with PPS-0-10 and PPS-2-10, which leads to the improvement of toughness. Figure 7 shows that PPS-4-10 and PPS-6-10 have much larger elongation at break and have necked phenomenon compared with PPS-2-10 and PPS-0-10, which means the former is tough and the later is brittle.

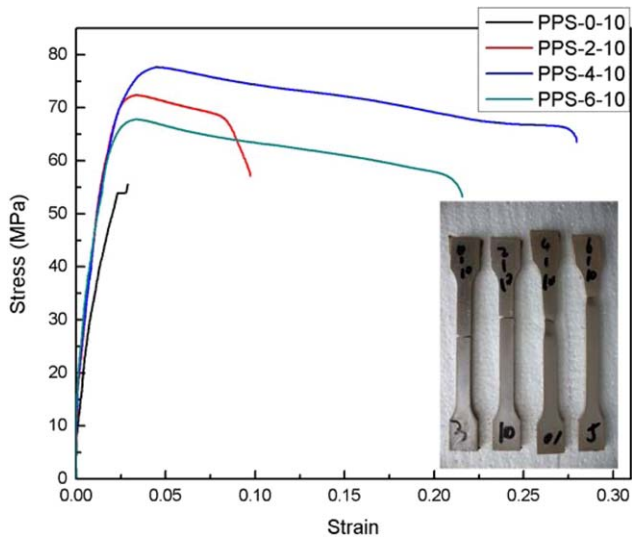

Figure 7. The stress–strain curves of PPS-0-10, PPS-2-10, PPS-4-10, and PPS-6-10. The bottom right is the tested specimens. The tensile speed was 1 mm/min. [Color figure can be viewed in the online issue, which is available at wileyonlinelibrary.com.]

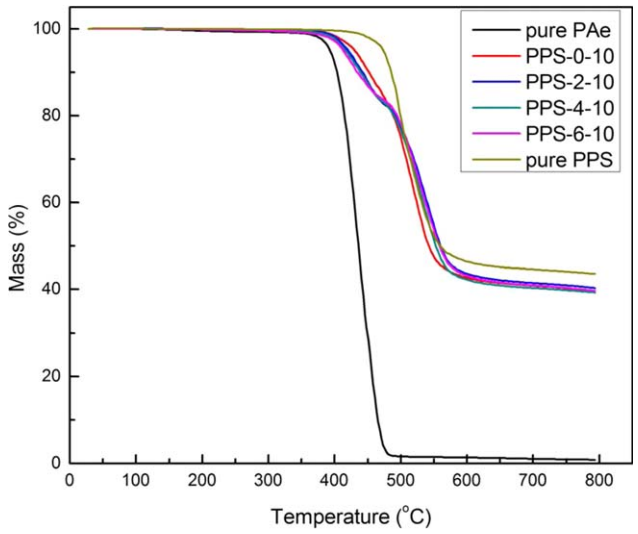

Figure 8. TGA curves of pure PAe, PPS-0-10, PPS-2-10, PPS-4-10, PPS-6-10, and pure PPS in nitrogen. [Color figure can be viewed in the online issue, which is available at wileyonlinelibrary.com.]

Thermostability of Blends

In Figure 8, the thermal decomposition of PPS/PAe/EP blends undergoes two stages. The lower decomposition temperatures are assigned to PAe, and the higher are assigned to PPS. The decomposition temperatures of PPS and PAe in PPS/PAe/EP system are almost identical with those of pure PPS and pure PAe. So the each component in PPS/PAe/EP system keeps its own thermostability.

Thermal Properties of Blends

In the literature, the value reported as the T_g, when using DMA measurements, varies with the onset of the E' drop, the peak of the tan δ, and the peak of the E''. In this article, the tan δ peak is used as the glass transition temperature. As shown in Figure 9, the glass transition temperature of PPS reduces with the addition of EP, which is beneficial to the toughness of blends. The heat deflection temperature also can indirectly reflect the glass transition temperature. It has the same trend with the glass transition temperature (shown in Table 3). These results can be easily explained. The addition of EP to PPS/PAe can improve their compatibility, so the glass transition temperature of PPS shifts to lower values.

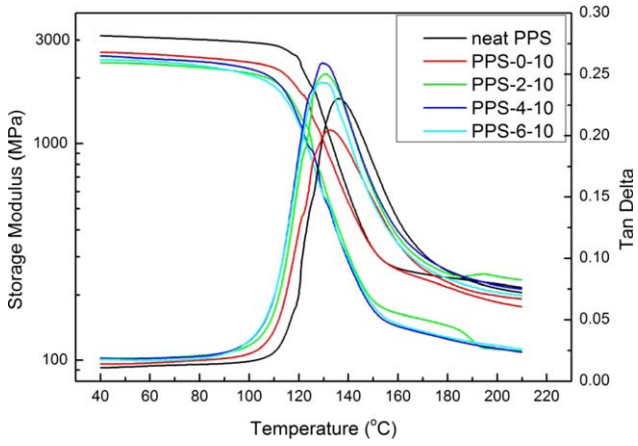

Figure 9. DMA results of neat PPS, PPS-0-10, PPS-2-10, PPS-4-10, and PPS-6-10. [Color figure can be viewed in the online issue, which is available at wileyonlinelibrary.com.]

Table 3. The Glass Transition Temperature (T_g) and the Heat Deflection Temperature (HDT) of Blend

	Pure PPS	PPS-0-10	PPS-2-10	PPS-4-10	PPS-6-10
T_g (°C)	136.0	132.8	130.7	129.5	129.2
HDT (°C)	105.0	102.8	99.2	97.5	96.8

CONCLUSIONS

The PPS/PAe/EP ternary blends were successfully prepared via reactive extrusion. The reactions among components are illustrated as follows.

1. The chain-extended reaction of PPS in the presence of EP. The chain-extended PPS can strengthen the tensile strength of blends, and it also benefits the toughness to some extent. Meanwhile, the improvement of the molecular weight of PPS also increases the viscosity, which is favorable to the extrusion and the blow molding.
2. The PPS-*g*-PAe reaction in the presence of EP. The PPS-*g*-PAe compatibilizer distributes in the interface between PPS and PAe, which can greatly enhance the interfacial adhesion and reduce the interfacial tension. It apparently has a positive effect on the tensile strength and impact strength.
3. The curing reaction of EP. The cured EP, which is immiscible with PPS, disperses in matrix as the stress concentration points and damages the mechanical properties of blends.

Compared with that of pure PPS, the mechanical properties of PPS/PAe/EP ternary system are improved, and their heat resistances are also preserved. Especially, when the weight ratio of PPS/PAe/EP is 100/10/4, the values of tensile strength, unnotched Charpy impact strength, and elongation at break reach their maximum, i.e. 77.7 MPa, 7.93%, and 75.69 kJ/m^2, respectively.

A toughened model for PPS/PAe/EP ternary system is proposed. The improvement of toughness for PPS/PAe/EP ternary system is ascribed to the active molecules which exist in the region of shear band. The shear band is brought out around dispersed particles and it is directly proportional to the superficial area of dispersed particles.

ACKNOWLEDGMENTS

This work was supported by the State Key Program of National Natural Science of China (Grant No. 50933004), and the National Natural Science Foundation of China (Grant No. 51003066). This work was also supported by the Young Scholars Foundation of Sichuan University (Grant No. 2008017), the Outstanding Young Scholars Foundation of Sichuan University (Grant No. 2011SCU04A13), and the Supporting Program for

New Century Excellent Talents in University of Ministry of Education of China (NCET-08-0368). This work was also supported by the Program for Changjiang Scholars and Innovative Research Team in University of Ministry of Education of China (IRT1026).

REFERENCES

1. Sugie, T.; Ishikawa, R.; Kobata, F. (to Dainippun Ink and Chemicals, Inc.). U.S. Pat. 4,528,346 (1985).
2. Choi, J.; Lim, S.; Kim, J.; Choe, C. *R. Polymer* **1997**, *38*, 4401.
3. Lee, S. L.; Chun, B. C. *Polymer* **1998**, *39*, 6441.
4. Chen, C. M.; Hsieh, T. E.; Liu, M. O. *React. Funct. Polym.* **2008**, *68*, 1307.
5. Cheung, M. F.; Plummer, H. K, Jr. *Polym. Eng. Sci.* **1996**, *36*, 15.
6. Wu, B.; Zheng, X.; Leng, J.; Yang, B.; Chen, X.; He, B. *J. Appl. Polym. Sci.* **2012**, *124*, 325.
7. Masamoto, J.; Kubo, K. *Polym. Eng. Sci.* **1996**, *36*, 265.
8. Hisamatsu, T.; Nakano, S.; Adachi, T.; Ishikawa, M.; Iwakura, K. *Polymer* **2000**, *41*, 4803.
9. Tang, W.; Hu, X.; Tang, J.; Jin, R. *J. Appl. Polym. Sci.* **2007**, *106*, 2648.
10. Kubo, K.; Masamoto, J. *J. Appl. Polym. Sci.* **2002**, *86*, 3030.
11. Lee, S. L.; Chun, B. C. *J. Mater. Sci.* **2000**, *35*, 1187.
12. Lee, B. S.; Chun, B. C. *Polym. Compos.* **2003**, *24*, 192.
13. Nam, J. D.; Kim, J.; Lee, S.; Lee, Y.; Park, C. *J. Appl. Polym. Sci.* **2003**, *87*, 661.
14. Zimmerman, D. A.; Koenig, J. L.; Ishida, H. *Spectrochim. Acta A* **1995**, *51*, 2397.
15. Kim, G. M.; Michler, G. H. *Polymer* **1998**, *39*, 5699.
16. Wu, S. *Polymer* **1985**, *26*, 1855.